2018 IEEE/RSJ International Conference on Intelligent Robots and Systems (IROS)
Madrid, Spain, October 1-5, 2018

# Development of Low-Inertia High-Stiffness Manipulator LIMS2 for High-Speed Manipulation of Foldable Objects*

Hansol Song, Yun-Soo Kim, Junsuk Yoon, Seong-Ho Yun, Jiwon Seo, and Yong-Jae Kim

***Abstract*—In this paper, a dual-arm robot system for high-speed manipulations, which is named LIMS2-AMBIDEX and is developed to compete in the IROS2018 Robotic Challenge, is presented. It has two seven-degrees-of-freedom (DOF) lightweight arms, a three-DOF head, and a one-DOF gripper to manipulate foldable objects. Because all the heavy actuators are placed at the shoulder, it has remarkably low mass beyond the shoulder (2.63 kg), which guarantees an inherent safety at high speeds. Utilizing tension-amplification mechanisms, the high stiffness and strength are achieved, and thus it has the control performance comparable to conventional industrial manipulators. A unique three-DOF wrist mechanism, whose motions directly represent the quaternion values of the joint orientation, can manipulate objects without singular points in the entire range of motion. In order to utilize the object's inertia during rapid manipulation, the gripper was specially designed: it has a one-DOF finger to grasp the upper rib of the foldable fan and two supporting forks to grasp the bottom rib stably.**

**For real-time performance and increased scalability, a software framework was developed based on Robot Operating System (ROS). The real-time capability is achieved by using the real-time development framework Xenomai and the high-speed communication protocol EtherCAT. As most of the algorithms are implemented in the distributed nodes using ROS, it is convenient to expand, improve, and replace the algorithms. Consequentially, the entire motion of the Fan Robotic Challenge Phase I Modality B required 1.05 s, which is substantially faster than a similar manipulation by most humans.**

## I. Introduction

Until the present, there have been various efforts to develop high-speed dexterous robots. For high-speed manipulation, fast and lightweight mechanisms and actuators as well as effective control algorithms with real-time software frameworks are required. Recently, as the demand for safe cooperative robots continuously increases, an increasing number of robots are appearing in markets and competitions. However, achieving safety during high-speed tasks by using conventional mechanisms and control systems is highly challenging.

Ishikawa *et al.* developed high-speed hand-arm systems using customized motors and gears [1,2]. Along with high-speed vision systems, these robots have exhibited remarkable results including actions such as hitting, catching, dribbling, and regrasping objects. Catching fast-flying objects is also a challenging and complex problem, which requires trajectory prediction, identification of optimal intercept points, and rapid trajectory planning [3]. Introducing softness in the catching approach and applying it to KUKA LWR4+, Sina *et al.* overcame the sensorimotor imprecision during catching [4].

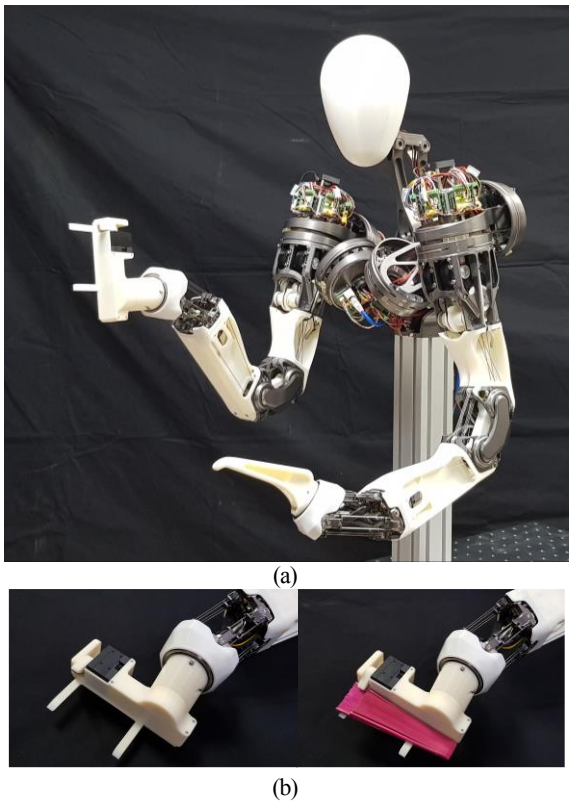

(a)

(b)

Fig. 1. (a) Developed dual-arm robot system LIMS2-AMBIDEX with a gripper on the right arm and a dummy hand on the left arm, (b) Developed Gripper for the fast manipulation of foldable objects.

In an environment where humans and robots operate together, safety is important apart from high accuracy and speed. Thus, an increasing number of researches on safety have also been carried out. A tendon-driven mechanism is suitable for minimizing robot mass and thus achieving safety during high-speed motions. The authors' previous work, the Low-Inertia High-Stiffness Manipulator LIMS1 [5], is also a tendon-driven robot. However, by introducing tension-amplification mechanisms, it accomplished high control performance comparable to the conventional industrial manipulators. An improved version of LIMS1, named LIMS2-AMBIDEX (LIMS2 for short), has a new wrist mechanism that represents the Quaternion relationship [6]. It

*Research supported by NAVER Labs. Co.

Yong-Jae Kim, is with Korea University of Technology and Education (Koreatech), Cheonan-City, Rep. of Korea (corresponding author to provide phone: +82-41-560-1424; fax: +82-41-564-3261; e-mail: yongjae@koreatech.ac.kr).

Hansol Song, Yun-Soo Kim, Junsuk Yoon, Seong-Ho Yun, Jiwon Seo, are with Korea University of Technology and Education (Koreatech), Cheonan-City, Rep. of Korea(e-mail: stan44@koreatech.ac.kr, yunsu335@koreatech.ac.kr,ynkb0401@koreatech.ac..kr,dnstjdgh@koreatech.ac.kr, aaeeghj@koreatech.ac.kr, scbw00@koreatech.ac.kr).

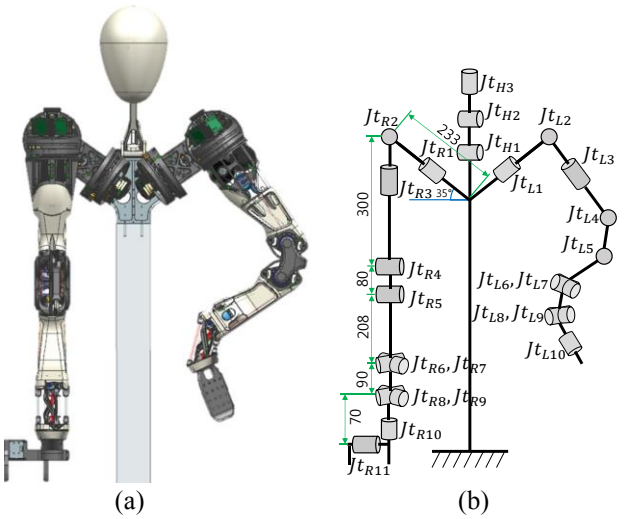


Fig. 2. Dimensions and joint placement of the LIMS2-AMBIDEX

exhibits a wide range of motion and maximum-manipulability measure in the entire range of motion, which is a useful property for fast and dexterous manipulation.

To develop a robot system for robot competitions, numerous important functionalities such as mechanical and control performance as well as system reliability and scalability and convenient development framework are required. The DARPA Robotics Challenge (DRC), funded by the US Defense Advanced Research Projects Agency and held from 2012 to 2015, is one of the most popular robotic competitions. Numerous articles including [7, 8] report the efforts and lessons-learned from the DRC experience. The IROS Fan Robotic Challenge is a robot manipulation competition where robots are required to manipulate the official foldable fan as effectively and rapidly as feasible. Two main features will score during this process: a) time and b) degree of opening and closing of the fan. The LIMS2 exhibits high speed and inherently safe characteristics suitable for the IROS Fan Robotic Challenge. For this competition, a gripper was specially developed to manipulate the foldable fan rapidly by using its inertia. Figure 1 shows the LIMS2 and the developed gripper. In addition, a software framework for LIMS2 was developed in ROS, enabling real-time control and convenient maintenance and expansion. Consequentially, the entire motion for the Fan Robotic Challenge Phase I Modality B required 1.05 s, which is substantially faster than most humans' manipulation time.

This paper is organized as follows: Section II describes the mechanical design of the improved robot LIMS2-AMBIDEX and its properties and performance. In Section III, the software framework for high-speed manipulation and the procedures of motions for the fan manipulation are explained. Section IV presents the experimental results, and Section V concludes with the summary and future work.

## II. Mechanical Design

### A. Specifications of LIMS2

Figure 2 illustrates the kinematic structure of LIMS2. Each arm has 10 joints. However, the motions of $Jt_{L/R4}$ and $Jt_{L/R5}$ at the elbow are coupled and exhibit one DOF, and similarly,

TABLE I
LIMS2-AMBIDEX Specifications

| Items | Specifications |
|---|---|
| Size and shape | 7 DOF per arm<br>- Shoulder 3 DOF, elbow 1 DOF, wrist 3 DOF |
| Mass | Arm moving part 2.63 kg<br>- Wrist : 446 g, Forearm : 171 g, Elbow : 533 g<br>- Upper arm (with wrist & elbow motors) :1,478 g<br>Shoulder : 4.17 kg |
| Range of motion (Right arm) | Shoulder pitch : -180 deg ~ 65 deg<br>Shoulder roll : -190 deg ~ 2 deg<br>Shoulder yaw : -95 deg ~ 170 deg<br>Elbow : -170 deg ~ 5 deg<br>Wrist roll, pitch : -90 deg ~ 90 deg<br>Wrist yaw : -300 deg ~ 300 deg |
| Speed | Shoulder roll, pitch : 499 deg/s<br>Shoulder yaw : 749 deg/s<br>Elbow : 590 deg/s<br>Wrist roll, pitch : 1,179 deg/s<br>Wrist yaw : 1,634 deg/s |

TABLE II
Gripper Specifications

| Items | Specifications |
|---|---|
| Size and shape | 1 DOF hand<br>- 1DOF 22.5mm finger |
| Mass | Whole hand part 208.3 g<br>- Actuator : 82 g Body : 126.3 g |
| Speed | Finger rotation : 46 rpm |
| Peak Torque | Finger rotation : 4.1 Nm |

the wrist joints from $Jt_{L/R6}$ to $Jt_{L/R9}$ are coupled to exhibit two DOFs. Thus, including the distal yaw joint $Jt_{L/R10}$, each wrist has three DOFs. Consequently, each arm exhibits seven DOFs. Tables I and II present the selected specifications of LIMS2 and the gripper, respectively. As is evident here, it has remarkably low mass and inertia, which are smaller than those of human arms, and exhibits a wide range of motion. Thus, it can assume more diverse postures than a human arm can. The gripper has a one-DOF finger, which can be regulated by reference angle with the adjustable maximum torque.

### B. Shoulder Design

Each shoulder exhibits three DOFs and a wide range of motion similar to human-like movements. As shown in Fig. 3 (c), the one-DOF actuators are stacked on the body frame in the order of the pitch, yaw, and roll joints. To prevent singularity near the frequently used configuration, the pitch joint has 35° of inclination (Figs. 2 (b) and 3 (c)).

The shoulder actuators were designed considering weight and inertia minimization, back-drivability and low friction, and the convenience of placement and harnessing of the electronics. The motors were newly customized to reduce the rotor inertia. They can exert a torque equivalent to those of LIMS1; however, the rotor inertia is six times smaller than the previous one. Each motor has a 10:1 low-backlash planetary gearhead. As shown in Figs. 3 (a) and (b), the capstan-drive mechanism provides additional reduction without increasing backlash and frictional loss. The shoulder contains four additional actuators (three for the three-DOF wrist and one for the one-DOF elbow), which aids in decreasing the rotational

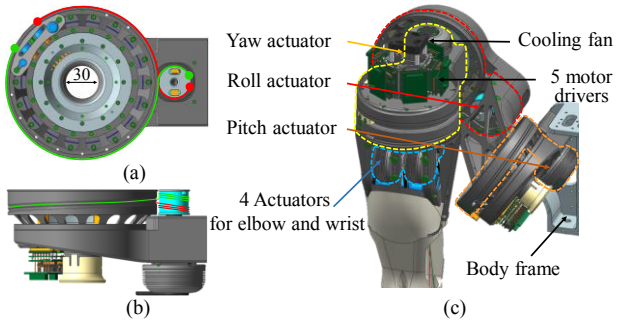


Fig. 3 Shoulder mechanisms. (a) Top view and (b) front view of shoulder actuator, (c) 3-DOF shoulder composed of three identical joint mechanisms.

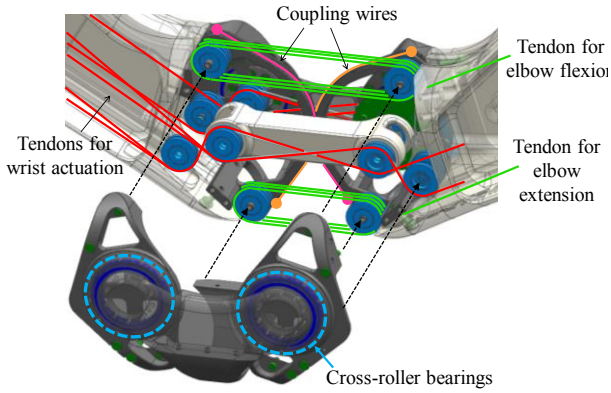


Fig. 4 Elbow mechanism

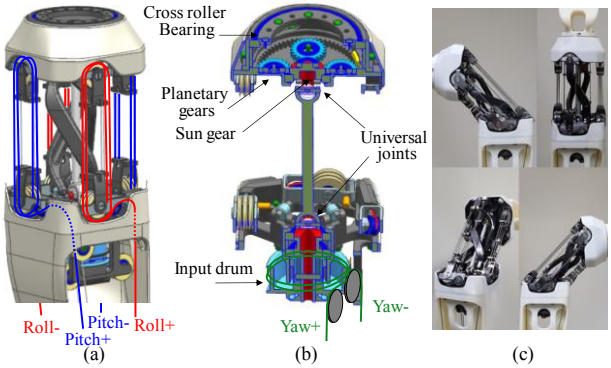


Fig. 5 Wrist mechanism, (a) paths of roll and pitch wire pairs, (b) wire routing and a planetary gear for additional reduction, (c) range of motion of the wrist by roll and pitch motions.

inertia of the whole arm. As shown in Fig. 3 (a), each shoulder actuator has a 30 mm diameter hole for electric cables, and five motor drivers are compactly attached on the yaw frame and can be conveniently cooled by a single cooling fan.

### C. Elbow Design

The elbow joint has a one-DOF rolling mechanism, wherein two coupling wires (pink and orange lines in Fig. 4) cause pure rolling between the two circular-contact shapes without slip. The flexion wire (upper green line) and extension wire (lower green line) come from the motor assembly (blue dotted area in Fig. 3 (c)) and wind around the pulleys at the forearm and the upper arm multiple times. Therefore, the wire tension is amplified by the number of winding. More

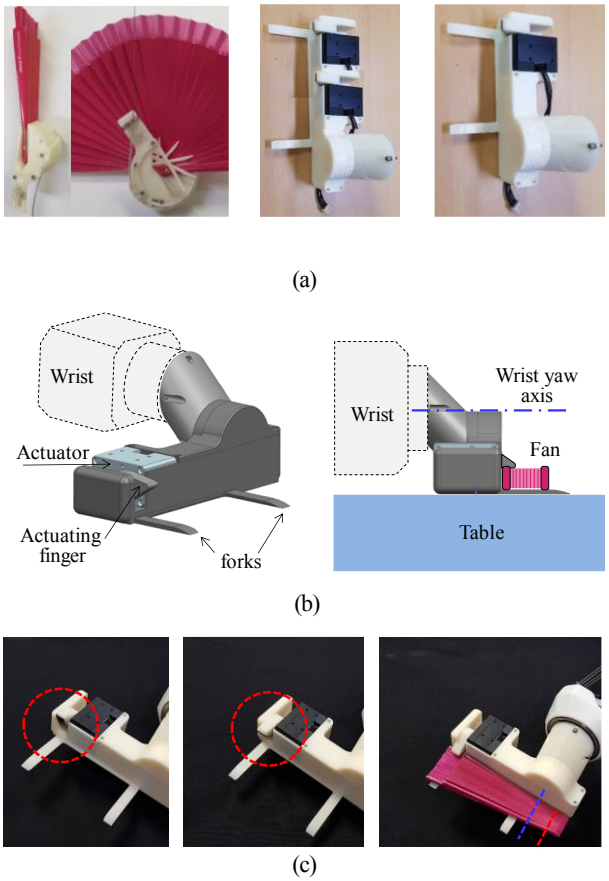


Fig. 6 Gripper mechanism: (a) an initial ideas, (b) final model, and (c) implemented gripper

importantly, the resultant joint stiffness is amplified by a quadratic order of the winding, which yields a high control performance. The wires for the wrist actuation (red lines) pass around the pulleys at the two centers of the rolling joint, which decouples the wire movement from the elbow motion. For the detailed description, refer to [5]. Although the fundamental concept is similar to that of LIMS1, numerous improvements have been incorporated. For example, four cross roller bearings are used to increase the strength and torsional stiffness of the elbow. The frames were designed to resemble an exoskeleton in order to contain complex tendon-transmitting mechanisms without interference or damage.

### D. Wrist Design

The wrist exhibits three DOFs, as mentioned in II.A. Figure 5 (a) shows the two-DOF part of the wrist with roll and pitch actuation wire pairs. It is the extended mechanism of the one-DOF rolling joint described in the previous subsection, to exhibit two DOFs. Rather than the circular-contact shapes of the one-DOF rolling joint, a unique three-link parallel mechanism approximates two-dimensional rolling motion between two hemispherical surfaces. By actuating the two wire-pairs roll+, roll- and pitch+, pitch-, the wrist can be bent in any direction. Figure 5(b) shows a section view of the mechanism for the distal yaw motion. The motion of the wire pair yaw+, yaw- is transmitted to the sun gear at the distal end of the wrist through two universal joints and a shaft. The planetary gears produce additional reduction ratio. As shown

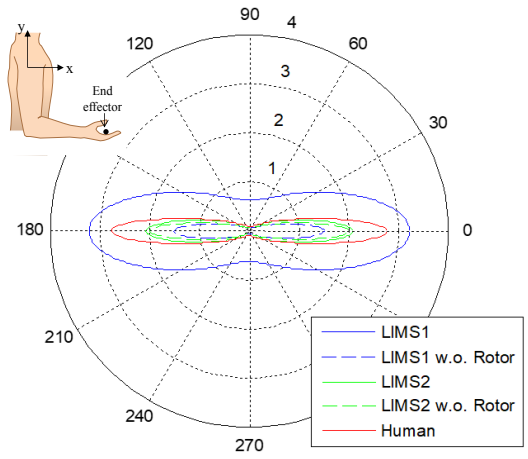


Fig. 7 Comparison of effective masses of LIMS1, LIMS2, and human arm (top left: configuration for effective mass calculation)

in Fig.5 (c), the roll and pitch motion have the range ± 90°, and the yaw motion has ± 300° in arbitrary directions without singular configurations.

### *E. Gripper Design*

At the initial stage of concept generation, several candidates for the gripper were considered. Figure 6 (a) shows three initial concepts. The left mechanism is composed of multiple layers of holding structures. It covers the bottom part of the fan, and when the fan opens, the layered structure rotates according to the opening of the fan, continuously covering the outside of the fan. The model at the center of Fig. 6 (a) has two fixed forks and two actuating fingers; thus, it can hold the fan securely. The rightmost model has two fixed forks and one actuating finger, which satisfies the requirement of the stable force closing without interfering with the opening of the fan and also exhibits the simplest structure. Therefore, considering the weight, simplicity, and holding capability, the last concept was selected.

As shown in Fig. 6 (b), the gripper has one DOF with a simple shape; however, it was developed by referring to a humans' rapid fan opening motion. It is designed to fulfill purposes of grasping, opening, and closing the fan. It has a flat bottom with two thin fixed forks to tightly contact with a table surface and to lift the fan on the table using the forks. The actuating finger can grasp the fan's outer guard. The length of the finger was properly determined in order not to hinder the motion of the ribs and leaves. The forks were designed to be replaceable in case of damage during the manipulation. Figure 6 (c) shows the implemented gripper. In order to use the inertia of the fan when opening and closing it, the axis of the wrist way and the pivot of the fan are designed to be close to each other. As shown in the rightmost picture of Fig. 6 (c), the pivot of the fan (red dotted line) is placed near the yaw axis of the wrist (blue dotted line).

### *F. Mechanical Properties and Performance*

As introduced in [5], the tension amplification mechanisms are applied to the elbow and the wrist to increase the stiffness and strength of the joints. In the case of the one-DOF elbow,

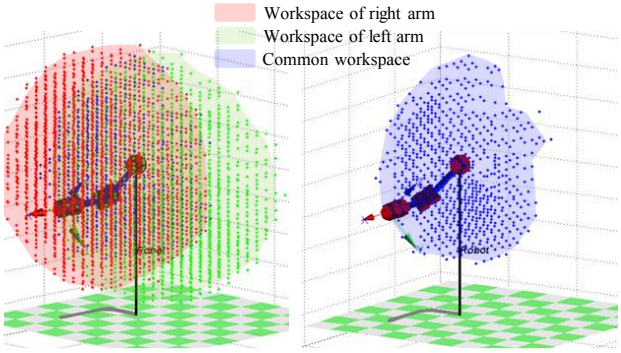


(a) (b)

Fig. 8 Dexterous workspace with respect to forward EE direction (a) workspace of left arm (green dots), right arm (red dots), and both arms (blue dot), (b) Common workspace of both arms

the displacements of the two antagonistic actuation wires, $l_{left}$ and $l_{right}$, have an identical magnitude albeit opposite directions, as indicated in the following:

$$l_{left} = -l_{right} = nwsin\frac{\theta}{2}, \tag{1}$$

where $n$ and $w$ denote the number of wire windings and the distance between the two antagonistic pulley centers, respectively. For the elbow joint shown in Fig. 4, $n$ and $w$ were set to 6 mm and 80 mm, respectively. Owing to this symmetric wire motion, the joint can be actuated with a single motor without slack or excessive tension. The maximum torque $\tau_{1DOF\ max}$ and the torsional stiffness $k_{1DOF}$ of the one-DOF joint mechanism are obtained as follows:

$$\tau_{1DOF\ max} = \left(\frac{nw}{2}cos\frac{\theta}{2}\right)T_{max}, \tag{2}$$

$$\kappa_{1DOF} = \left(\frac{n^2w^2}{2}cos^2\frac{\theta}{2}\right)k_{wire}, \tag{3}$$

It is noteworthy that the stiffness can be amplified by the quadratic order of $n$. The same concept can be extended to the two-DOF bending joint for the wrist, as shown in Fig.5 (a). The relationship between the bending pose $(\phi, \theta)$ and the motion of the wire pair $(l_r, l_p)$ can be obtained as

$$l_r = {l_r}^+ = -{l_r}^- = nw\sin\phi\sin\frac{\theta}{2}, \tag{4}$$

$$l_p = {l_p}^+ = -{l_p}^- = nw\cos\phi\sin\frac{\theta}{2}, \tag{5}$$

which illustrates that the motions of the wire pairs are also completely symmetrical. Here, n and w for the wrist are 4 and 69 mm, respectively. Similar to (3), the stiffness of the two-DOF joint is also amplified by the quadratic order of $n$. For a detailed explanation, refer to [5]. One of the unique properties of the wrist is that the motions of the wire pair $(l_r, l_p)$ directly represent the quaternion values of the joint orientation. The wrist orientation can be represented by the unit quaternion as follows:

$$q_Q = < \eta_Q, \epsilon_Q > = < \eta, r, p, 0 >, \tag{6}$$

where $r = \frac{l_r}{nw}$, $p = \frac{l_p}{nw}$, and $\eta = \sqrt{r^2 + p^2}$.

For further explanation, refer to [6].

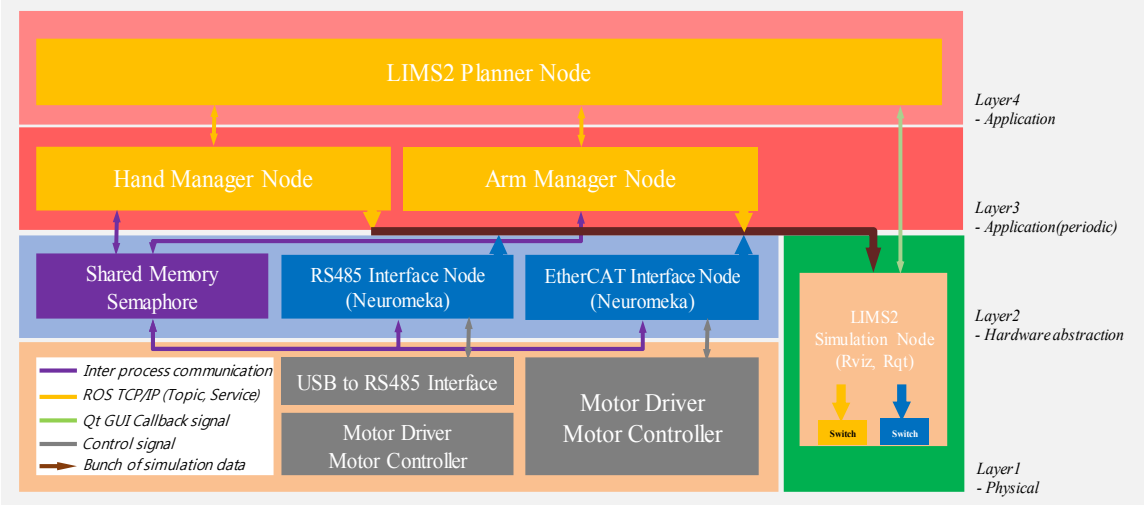


Fig. 9 Software Framework for LIMS2

As aforementioned, LIMS2 has customized motors with a substantially smaller rotor inertia (28.7 g·cm$^2$) than that of the previous robot LIMS1 (181g·cm$^2$). It significantly influences the effective mass of the arms. Figure 7 illustrates the effective mass of the end-effector at the pose shown at the top left of the figure for several cases: LIMS1 with/without motor rotors, LIMS2 with/without motor rotors, and human arms. As shown in the figure, the effective masses of LIMS1 with and without motor rotors (solid blue curve and dashed blue curve) exhibit a substantial difference, which implies that the rotor inertia can be the most dominant mass factor in lightweight mechanisms because the rotor inertia is amplified by a quadratic order of the gear ratio. However, LIMS2 with the improved motors (dashed green curve) has a smaller effective mass than the human arm (red curve).

Figure 8 (a) shows the workspace of the LIMS2 with the end-effector oriented toward the front. Because of the compact size and large range of motion of the wrist, each arm has a large workspace. Moreover, the robot has a large common area of workspace of the two arms, as shown in Fig. 8 (b); this is indispensable for two-arm manipulations.

## III. Control System for High-Speed Manipulation

The control system for high-speed manipulation was developed based on Robot Operating System (ROS). ROS is a software framework, which is already widely in use in the field of robotics and is a useful middleware in Linux for developing robots. Because the ROS can manage large control systems by multiple distributed modular processes (termed as nodes) and provides convenient communication tools between the nodes, the system can be conveniently maintained and expanded. In order to achieve real-time capability, the real-time development framework Xenomai and the high-speed communication protocol EtherCAT are used as it was necessary to transmit commands to 17-axes manipulators at high speed.

### *A. Software Framework for LIMS2*

Figure 9 illustrates the software framework for LIMS2. The framework is composed of four layers; an application layer (Layer 4), a manager layer (Layer 3), a hardware abstraction layer (Layer 2), and a physical layer (Layer 1). Each layer contains one or multiple nodes and other real-time processes or drivers.

Layer 4 has *LIMS2 Planner Node,* which makes a decision for an assigned task and intermittently transmits commands to the *Manager Nodes*. This planner node can be replaced according to the tasks. The most important role of the planner node for the Fan Robotic Challenge is to manage the motion sequence of each arm and to transmit the target motions to the managers at the appropriate time. That is, the planer node transmits information including the motion type (e.g. point-to-point or linear in Cartesian space), acceleration and deceleration time, moving time, and desired joint angles or end-effector pose. Moreover, after the moving time, it transmits the next information according to the task procedure, as shown in Fig. 10.

Layer 3 has two Manager Nodes, *Arm Manager* and *Hand Manager*, which are operated in real time. Because most of the algorithms requiring periodic calculation are operated in this layer, each manager node has a real-time loop; the Arm manager and Hand manager have 3-ms and 10-ms loops, respectively. Each manager node calculates the forward and inverse kinematics, Jacobian, motion trajectories, etc. based on the commands received from the planner node and the information received from the hardware abstraction layer.

Hardware abstraction layer, Layer 2, contains Shared Memory and Semaphore. Because the TCP/IP protocol provided by ROS can cause a delay or malfunction, Shared Memory, which is one of the IPC (Inter Process Communication) regulated by the kernel, is used to manage the data shared between the manager nodes. Simultaneously, a Semaphore is used in conjunction with the shared memory to avoid sync problems. There are two interface nodes operated in real-time loops, EtherCAT Interface Node and RS485 Interface Node; these are used in conjunction with the real-time operating system (Xenomai) to ensure the rapid movement and correct control cycles of the Manager Nodes. These interface nodes play the role of the bridge between the

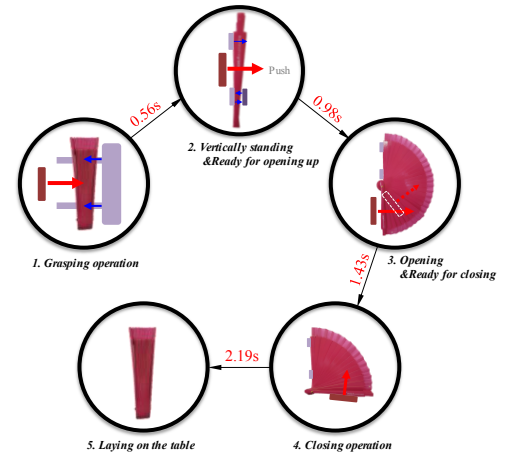


(a)

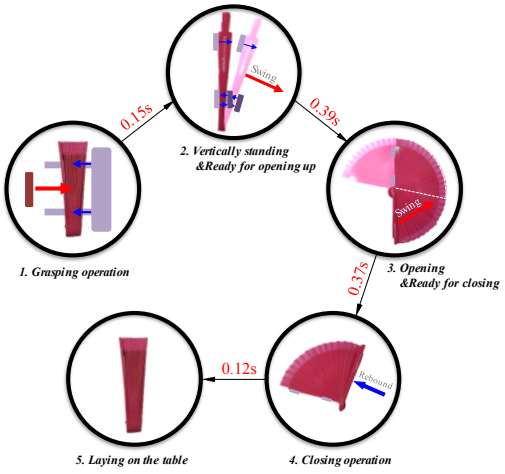


(b)

Fig. 10 (a) Two-hand fan manipulation procedure (b) one-hand fan manipulation procedure

actual hardware at the physical layer (Layer 1) and the manager algorithms using idealized hardware data.

As shown in the connections between Layers 2 and 3 (the thick red line), one can switch between the simulation and the actual robot operation without modifying the system architecture. Therefore, the users can conveniently examine the feasibility of the robot motions prior to the actual robot operation.

### *B. Motion Generation for Fan Manipulation*

Two types of motions of the fan manipulation were implemented; two-hand manipulation and one-hand manipulation. Figure 10(a) shows the procedure for the two-hand manipulation. It was designed to pick up the fan securely and to open and close it using both the hands, with the aid of gravitational force. Firstly, the gripper of the right arm and the dummy hand of the left arm stay marginally in contact with the table, and the fan lies between the two grippers. The dummy hand pushes the fan to the gripper, and then, the gripper holds the fan using the two forks and a finger. Subsequently, the right arm raises the fan vertically, and the dummy hand on the left arm shifts to the position between the


(a)


( b)

Fig. 11 Snapshots of experiment. (a) 1-hand manipulation (b) 2-hand manipulation

gripper's two forks to help open the fan. By pushing the fan diagonally with the dummy hand as shown in Fig. 10(a) with the assistance of the gravity, the fan is opened. To close it, the gripper leans forward, and the dummy hand pushes back the ribs of the fan along the arc curve following the fan shape. Finally, the robot places the closed fan on the table.

The one-hand manipulation has an identical procedure except for the opening and closing motions. As shown in Fig. 10(b), these motions are conducted by using only the gripper on the right arm. The wrist rapidly rotates to the forward and reverse directions as shown in steps 3 and 4 in the figure. Owing to the inertia of the fan and the rapid wrist motion, complete opening and closing are achieved. To reduce the time for the whole procedure, the target pose and motion profile of each step were carefully selected considering the minimum distance of the trajectory and the efficient use of the lightweight and high-speed characteristics of LIMS2.

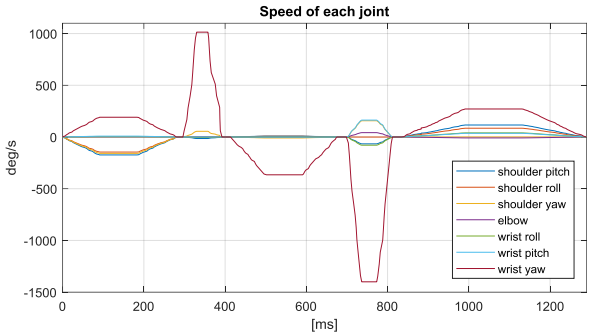


(a)

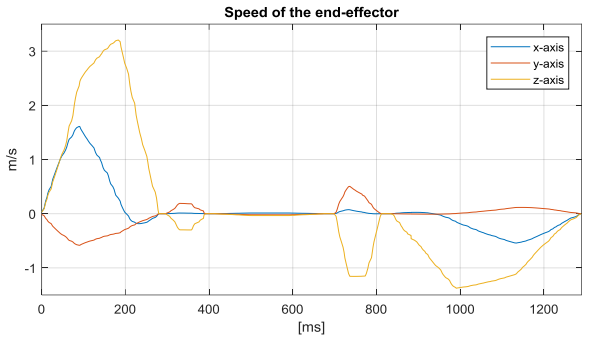


(b)

Fig. 12. Target speed of robot in joint space and Cartesian space of right arm for one-hand manipulation. (a) Speed of each joint in joint space. (b) Speed of end-effector in Cartesian space.

Particularly, the redundant DOFs of the arms were set to minimize the motion of the relatively heavy upper arms.

The generated operation time was 1.05 s, which is the elapsed time from the moment of the first contact of the dummy hand with the fan to the moment that the fan leaves the gripper. It is significantly faster than the two-hand manipulation and most humans' manipulation.

## IV. Experimental Result

The experiments for the two-hand and one-hand manipulations were performed. As the two-hand manipulation uses both the hands for the opening and closing, it could perform the tasks stably regardless of the fan condition or disturbance. As shown in Fig. 11(a), when opening and closing the fan, the gripper of the right arm rotates the fan, and, simultaneously, the dummy hand of the left arm pushes the other side of the fan in the opposite direction. As the closing motion is relatively slow, occasionally, the fan does not close completely. Thus, additional pushing motion at the horizontal pose of the fan was added right after finishing the first closing motion (bottom left picture in Fig. 11(a)). The total operation time was 5.16 sec.

Although the two-hand manipulation is stable, it has a limited speed because of the numerous conservative and even unnecessary motions. The one-hand manipulation was performed as shown in Fig. 11(b). Repeated experiments had verified the effectiveness of this strategy, and the resultant operation time was reduced to 1.05 s.

Figure 12 (a) shows the target joint speed of the right arm for the one-hand manipulation. It is demonstrated that the speed of the wrist yaw varies significantly from approximately 300 to 800 ms. The first positive peak and the second negative peak of the wrist yaw speed indicate the opening movement. The third negative peak value (from 700 ms to 800 ms) induces the closing motion. To close the fan completely by applying high acceleration to the fan, almost the maximum speed of the yaw joint was used in this motion. The fastest angular velocity in this section is 1400°/s. As shown in Fig. 12(b), the fastest instantaneous velocity of the end-effector is 3.2 m/s.

## V. Conclusion and Future Work

This paper presented the mechanical design, hardware properties, and control system design of a dual-arm robot system for high-speed object manipulations for participating in the IROS Fan Robotic Challenge. The developed robot, named LIMS2-AMBIDEX, is the improved version of a low-inertia high-stiffness manipulator LIMS2. The overall design and the improved actuators and mechanisms were explained in detail, and the software framework developed considering real-time performance and expandability was introduced. Because of its remarkably low arm-inertia, the robot could complete the whole manipulation task successfully in 1.05 s, which is considered faster than a similar manipulation by most humans.

For further work, the research on the dynamic human motions such as dart throwing or catching fast objects will be conducted and applied to the robot. In addition, a high DOF waist mechanism is undergoing development in order to increase the workspace and enable safe and agile whole body motions.

## Acknowledgment

The authors would like to thank NAVER Labs Corporation for their support.

## References

[1] A. Namiki, Y. Imai, M. Ishikawa, and M. Kaneko, "Development of a high-speed multifingered hand system and its application to catching," *IEEE/RSJ Int. Conf. Intell. Robot. Syst.* (IROS), pp. 2666-2671, Oct. 2003.

[2] Y. Yamakawa, A. Namiki, and M. Ishikawa, "Dexterous manipulation of a rhythmic gymnastics ribbon with constant, high-speed motion of a high-speed manipulator," *IEEE Int. Conf. Robot. Automation* (ICRA), pp. 1896-1900, 2013.

[3] S. Kim, A. Shukla, and A. Billard, "Catching Object in Flight," *IEEE Trans. Robot.*, Vol.30, No. 5, pp. 1049-1065, 2016.

[4] S. Sina, M. Salehian, M. Khoramshahi, and A. Billard, "A Dynamical System Approach for Softly Catching a Flying Object: Theory and Experiment," *IEEE Trans. Robot.*, Vol.32, No. 2, pp. 462-471, 2016.

[5] Y-J. Kim, "Anthropomorphic Low-Inertia High-Stiffness Manipulator for High-Speed Safe Interaction," *IEEE Trans. Robot.*, Vol. 33, Issue 6, Aug. 2017.

[6] Y-J. Kim, J-I. Kim, and W. Jang, "Quaternion Joint: Dexterous 3-DOF Joint Representing Quaternion Motion for High-Speed Safe Interaction," *IEEE/RSJ Int. Conf. Intell. Robot. Syst. (IROS)*, submitted, 2018.

[7] T. Jung, J. Lim, H. Bae, K. K. Lee, H.-M. Joe, and J.-H. Oh, "Development of the Humanoid Disaster Response Platform DRC-HUBO+," *IEEE Trans. Robot.*, Vol. 34, Issue 1, Feb. 2018.

[8] C. Knabe, J. Seminatore, J. Webb, M. Hopkins, T. Furukawa, A. Leonessa, and B. Lattimer, "Design of a Series Elastic Humanoid for the DARPA Robotics Challenge," *2015 IEEE-RAS 15th Int. Conf. Humanoid Robot.*, pp. 738-743, Dec. 2015.